Local Approximations to the Gravitational Collapse of Cold Matter

Lam Hui and Edmund Bertschinger

Department of Physics, Massachusetts Institute of Technology

Cambridge, MA 02139

ABSTRACT

We investigate three different local approximations for nonlinear gravitational instability in the framework of cosmological Lagrangian fluid dynamics of cold dust. By local we mean that the evolution is described by a set of ordinary differential equations in time for each mass element with no coupling to other mass elements aside from those implied by the initial conditions. We first show that the Zel'dovich approximation (ZA) can be cast in this form. Next we consider extensions involving the evolution of the Newtonian tidal tensor. We show that two approximations can be found that are exact for plane-parallel and spherical perturbations. The first one ("non-magnetic" approximation, or NMA) neglects the Newtonian counterpart of the magnetic part of the Weyl tensor in the fluid frame and was investigated previously by Bertschinger & Jain (1994). A new approximation ("local tidal", or LTA) involves neglecting still more terms in the tidal evolution equation. It is motivated by the analytic demonstration that it is exact for any perturbations whose gravitational and velocity equipotentials have the same constant shape with time. Thus, the LTA is exact for spherical, cylindrical, and plane-parallel perturbations. We tested all three local approximations in the case of the collapse of a homogeneous triaxial ellipsoid, for which an exact solution exists for an ellipsoid embedded in empty space and an excellent approximation is known in the cosmological context. We find that the LTA is significantly more accurate in general than the ZA and the NMA. Like the ZA, but unlike the NMA, the LTA generically lead to pancake collapse. For a randomly chosen mass element in an Einstein-de Sitter universe, assuming a Gaussian random field of initial density fluctuations, the LTA predicts that at least 78% of initially underdense regions collapse owing to nonlinear effects of shear and tides.

Subject headings: cosmology: theory — dark matter — gravitation — large-scale structure of universe

1. Introduction

The complexity of nonlinear gravitational instability challenges our understanding of the universe. Even though the law of gravity between two bodies is very simple in the non-relativistic limit, the long-range interactions among exceedingly many bodies leads to behavior that defies simple analysis beyond the linear regime. Computer simulation with N-body methods provides a comprehensive approach to this problem, but it suffers from finite dynamic range and computational expense. Even more importantly, simulations do not increase our understanding of dynamics without guidance from analytical approaches.

In this paper, we explore a class of what we call local approximations for the nonlinear dynamics of self-gravitating cold matter. By local we mean that each mass element behaves as if it evolves independently of all the others once the initial conditions are specified. This might sound quite implausible. After all, mass elements do influence each other through gravity. However, as we will demonstrate, the celebrated Zel'dovich (1970) approximation (henceforth ZA) can be viewed as exactly an approximation of this sort.

In the past several years, there have been various attempts to improve upon the ZA, including the adhesion approximation (Kofman, Pogosyan, & Shandarin 1990), the frozen flow approximation (Matarrese et al. 1992), the frozen potential approximation (Brainerd, Scherrer, & Villumsen 1993; Bagla & Padmanabhan 1994), the truncated Zel'dovich approximation (Coles, Melott, & Shandarin 1993), and higher-order Lagrangian perturbation theory (Melott, Buchert, & Weiss 1995) (note that the ZA can also be regarded as the first-order solution in Lagrangian perturbation theory). Most of them are attempts to deal with the evolution of high density regions after trajectories cross, when the ZA ceases to be adequate. However, this is a difficult problem. Aside from the spherical model (Peebles 1980) and its cousins, there still exists little in the way of approximations methods for post-collapse evolution.

In this paper, we will not try to tackle the problem of trajectory crossing or the subsequent nonlinear evolution. Instead we ask whether one can improve upon the ZA even before orbits cross by seeking generalizations of the ZA within the framework of local approximations. In simple terms, a local approximation is one in which the evolution of each mass element is described by a set of ordinary differential equations in time in which there is no coupling to other mass elements, aside from those implied by the initial conditions. For instance, as we will explain more fully later, the evolution of a given mass element under the ZA is completely determined once the initial expansion, vorticity, shear and density at this mass element are specified. (The first three quantities correspond to the trace, antisymmetric part and traceless symmetric part of the velocity gradient tensor.) The evolution of other mass elements have no effect on the evolution of these quantities

at this mass element. In other words, under the ZA, all the information about other mass elements is encoded in the initial conditions. Once these are specified, each mass element goes for its own "free ride"!

We shall seek generalizations of the ZA by first systematically writing down a set of Lagrangian evolution equations for the velocity and gravity gradient for a given fluid element. We discuss two local approximations based on ignoring certain terms in the evolution equation for the Newtonian tidal tensor. One of them was introduced by Bertschinger & Jain (1994). They used the fact that if a quantity known as the magnetic part of the Weyl tensor vanishes in the Newtonian limit, the set of exact Lagrangian fluid equations for cold dust becomes local. (This fact was proven in general relativity by Matarrese, Pantano, & Saez 1993 following earlier work of Barnes & Rowlingson 1989; part of the motivation for such an assumption was the statement of Ellis 1971 that there is no counterpart to the magnetic part of the Weyl tensor in Newtonian theory.) Bertschinger & Jain then obtained the result that spindle (filamentary) collapse is favored in general as opposed to pancake collapse. (Pancake collapse had been thought — correctly — to be the generic outcome of gravitational collapse of cold dust following the work of Zel'dovich 1970.) Since then, it has been shown that the magnetic part of the Weyl tensor does have a Newtonian counterpart (Bertschinger & Hamilton 1994; Kofman & Pogosyan 1995 obtained equivalent results but describe their conclusions slightly differently). Until now, there has been no quantitative determination of the magnetic Weyl term neglected by Bertschinger & Jain in the tidal evolution equation. With reasonable assumptions, this term may be negligible on super-horizon scales, leading to "silent universes" (Bruni, Matarrese, & Pantano 1995).

Our second local approximation based on the tidal evolution equation is entirely new. It is based on dropping several more terms in addition to the Weyl tensor term. We will show why this is a better approximation compared to the one proposed by Bertschinger & Jain (1994). In fact, in tests this new approximation performs even better than the ZA, both in cases where exact solutions are known and where numerical solutions are calculated. In this paper, we concentrate on a comparison of the three local approximations for ellipsoids, with and without symmetries.

To understand the main ideas underlying these local approximation methods, and how they differ from other approaches, it is useful to draw an analogy with gravitational lensing. Our use of Lagrangian fluid equations is akin to solving the optical scalar equations (Sachs 1961), whereby one follows the two-dimensional cross-section of a congruence of light rays propagating through space. Our approach is similar, with light rays replaced by cold dust, and with the two-dimensional cross-section replaced by the three-dimensional volume of a

mass element. In fact, both approaches follow from the pioneering work in general relativity by Ehlers (1961) and Kundt & Trümper (1961). The first application of these methods to matter was by Hawking (1966), who pioneered the covariant fluid approach to cosmological perturbation theory. The formalism was championed by Ellis (1971) and eventually was applied to the formation of large scale structure (Bertschinger 1995 and the references cited previously). As in the case of gravitational lensing, this approach can tell how a given (mass) element evolves but does not give its trajectory. The optical scalar equations do not replace the gravitational lens equation, they supplement it. Likewise, the local methods we advocate can supplement N-body simulations or other approximations such as Lagrangian perturbation theory, by providing accurate ways to follow the deformation of mass elements as they evolve under gravity.

The organization of the paper is as follows. In §2, we show how the ZA is a local approximation. Section 3 presents two additional local approximations based on dropping terms from the tidal evolution equation, and shows under what circumstances these approximations are exact. To compare the three different local approximations for more general initial conditions, in §4 we consider the motion of a homogeneous ellipsoid, in both cosmological (Friedmann-Robertson-Walker background) and noncosmological (vacuum) contexts. The Weyl tensor and other relevant terms in the tidal evolution equation are evaluated. In §5 we discuss how different nonlinear approximations predict pancake versus spindle collapse from generic initial conditions, for which we also calculate the collapse times. Conclusions are presented in §6. The Appendix presents some results of second-order perturbation theory.

2.   On the Zel'dovich Approximation

In this section we review the Zel'dovich approximation starting from the Eulerian fluid equations in comoving coordinates. We then show that it can be regarded as a local approximation.

The cosmological fluid equations for cold dust in a perturbed Robertson-Walker universe with expansion scale factor $a(\tau)$ are (Bertschinger 1995):

$$\frac{\partial \delta}{\partial \tau} + \nabla_i \left[(1+\delta)v^i \right] = 0 \ , \tag{1}$$

$$\frac{\partial v^i}{\partial \tau} + v^j \nabla_j v^i = -\frac{\dot{a}}{a} v^i - \nabla^i \phi \ , \tag{2}$$

$$\nabla^2 \phi = 4\pi G a^2 \bar{\rho} \delta \ . \tag{3}$$

The mass density is $\rho = \bar{\rho}(\tau)(1 + \delta)$ and $\vec{v} = d\vec{x}/d\tau$ is the proper peculiar velocity where $\vec{x}$ is the comoving spatial position and τ is the conformal time (hence, $d\tau = dt/a$ where t is the proper time). We are neglecting spatial curvature so that we can use Cartesian coordinates where $\nabla^i = \nabla_i = \partial/\partial x^i$ for the ith spatial coordinate.

The trajectory of a fluid element is $x^i(\vec{q}, \tau)$ where $\vec{q}$ is a Lagrangian coordinate labeling the element, conventionally chosen to be the initial position:

$$x^i(\vec{q}, \tau) = q^i + \psi^i(\vec{q}, \tau) \ . \tag{4}$$

Now we introduce the Lagrangian time derivative $d/d\tau \equiv \partial/\partial\tau + v^j\nabla_j$. This time derivative commutes with $\partial/\partial q^i$. Using $v^i = d\psi^i/d\tau$, we can rewrite equation (2) as

$$\frac{d^2}{d\tau^2}\psi^i + \frac{\dot{a}}{a}\frac{d}{d\tau}\psi^i - 4\pi G a^2 \bar{\rho}\psi^i = -\nabla^i\phi - 4\pi G a^2 \bar{\rho}\psi^i \ . \tag{5}$$

Each term on the left-hand side is first order in ψ^i. The right-hand side can be estimated from the Poisson equation (3), but first we need the mass density. It follows in the Lagrangian approach by noting that ρd^3x is conserved along a fluid streamline provided d^3x is computed from the mapping $\vec{q} \to \vec{x}$. If there are no displacements, $\vec{q} = \vec{x}$ and $\rho = \bar{\rho}$. The volume element follows from the Jacobian determinant, leading to

$$\rho(\vec{q}, \tau) = \bar{\rho} \left| \frac{\partial x^i}{\partial q^j} \right|^{-1} \ . \tag{6}$$

For small displacements the Jacobian may be expanded in a power series; the first-order term gives $\rho = \bar{\rho}(1 - \partial\psi^i/\partial q^i) + O(\psi^2)$. Now note that $\partial\psi^i/\partial x^i = (\partial\psi^i/\partial q^j)(\partial q^j/\partial x^i) = \partial\psi^i/\partial q^i + O(\psi^2)$. Therefore, using equation (3), we see that the divergence of the right-hand side of equation (5) vanishes to first order in ψ^i. If ψ^i is longitudinal (i.e., has vanishing curl), then the right-hand side itself vanishes to first order. Displacements that grow by gravity are necessarily longitudinal in linear theory. The ZA consists of setting to zero the right-hand side of equation (5). (It can be generalized to allow for a transverse displacement; see Buchert 1993 and Barrow & Saich 1993.) Under the ZA, the evolution of displacement thus obtained is used in equation (6) to get the density field. The ZA is equivalent to first order Lagrangian perturbation theory for the trajectories $\vec{x}(\vec{q}, \tau)$.

With vanishing right-hand side, equation (5) is identical to the linear perturbation evolution equation for δ (a fact that becomes obvious when one notes $\delta = -\partial\psi^i/\partial q^i$ and $d/d\tau = \partial/\partial\tau$ to first order in ψ). This second-order ordinary differential equation in time has two independent solutions that we write $D_\pm(\tau)$ (Peebles 1980). Taking the growing

solution and requiring ψ^i to be longitudinal, we get the solution

$$\psi^i(\vec{q}, \tau) = D_+(\tau)\frac{\partial \varphi(\vec{q})}{\partial q^i} \tag{7}$$

where $\varphi(\vec{q})$ is a displacement potential which is fixed by initial conditions.

Next we will show that equations (4) and (7) imply that the ZA displacement field is longitudinal in x-space (the irrotational initial conditions already imply it is irrotational in q-space), a first step needed before we show that the ZA is a local approximation. We have

$$\left(\vec{\nabla} \times \vec{\psi}\right)_i = D_+(\tau)\epsilon_{ijk}\frac{\partial}{\partial x^j}\left(\frac{\partial \varphi}{\partial q^k}\right) = D_+\epsilon_{ijk}\left(\frac{\partial q^l}{\partial x^j}\right)\left(\frac{\partial^2 \varphi}{\partial q^k\,\partial q^l}\right) \ ,$$

where ϵ_{ijk} is the usual antisymmetric Levi-Civita symbol. Now, note that the Jacobian matrix defined by the transformation of equations (4) and (7), $\partial x^j/\partial q^l = \delta_{jl} + D_+\partial^2\varphi/\partial q^j\,\partial q^l$, is real and symmetric. By a theorem of linear algebra its inverse, $\partial q^l/\partial x^j$, is also symmetric. So is $\partial^2\varphi/\partial q^k\,\partial q^l$ and, because they commute, so is their product. Thus, in the equation for $\vec{\nabla} \times \vec{\psi}$ above, ϵ_{ijk} is contracted with a matrix that is symmetric in j and k, yielding $\vec{\nabla} \times \vec{\psi} = 0$ (Zel'dovich & Novikov 1983).

The implication of this result is that $\vec{\psi}$ is longitudinal in $\vec{x}$-space as well as in $\vec{q}$-space. The same conclusions hold for the velocity field $\vec{v}$, since it differs from $\vec{\psi}$ by only a time-varying factor $\dot{D}_+/D_+$. As a result, under the Zel'dovich approximation we can write

$$\psi^i(\vec{q}(\vec{x}, \tau), \tau) = D_+(\tau)\frac{\partial \Phi(\vec{x}, \tau)}{\partial x^i} \quad \text{and} \quad v^i(\vec{x}, \tau) = \dot{D}_+(\tau)\frac{\partial \Phi(\vec{x}, \tau)}{\partial x^i} \ ; \quad \frac{d\Phi(\vec{x}, \tau)}{d\tau} = 0 \ . \tag{8}$$

The last equation follows from the fact that $\partial\Phi/\partial x^i = \partial\varphi/\partial q^i$ (cf. eq. 7). Recall that under the ZA the right-hand side of equation (5) vanishes. Using equation (8), we then get

$$\vec{v} = -\dot{D}_+\left(4\pi Ga^2\bar{\rho}D_+\right)^{-1}\vec{\nabla}\phi = -\frac{2\dot{a}\,f}{3\Omega_0 H_0^2}\vec{\nabla}\phi \ , \tag{9}$$

where $f \equiv d\ln D_+/d\ln a$. Thus, in the Zel'dovich approximation, the velocity field is always (not just to first order in $\vec{\psi}$) proportional to the gravity field (Kofman 1991). It is clear geometrically that this result must be correct for planar, cylindrical, or spherical flow for growing mode initial conditions. For plane-parallel flows, but not otherwise, the coefficient of proportionality of the ZA is also correct, so that the ZA is exact (until orbit-crossing) in one dimension.

We are now going to present the ZA from another point of view. Similar work has been done by Kofman & Pogosyan (1995). Our aim is to motivate how one might improve

the ZA by generalizing it to a broader class of local approximations. It will become clear shortly exactly what we mean by local approximations.

Let us first give a brief summary of the Lagrangian fluid equations (Bertschinger & Jain 1994). First of all, the gradient of the fluid velocity field is decomposed into its trace, traceless symmetric and antisymmetric parts, which are the expansion θ, shear σ_{ij} and vorticity ω_{ij} respectively:

$$\nabla_i v_j = \frac{1}{3}\theta\,\delta_{ij} + \sigma_{ij} + \omega_{ij} \quad \sigma_{ij} = \sigma_{ji} , \quad \omega_{ij} = \epsilon_{ijk}\,\omega^k = -\omega_{ji} , \tag{10}$$

where $2\vec{\omega} = \vec{\nabla} \times \vec{v}$. Then, converting time derivatives from Eulerian to Lagrangian, equation (1) becomes

$$\frac{d\delta}{d\tau} + (1 + \delta)\,\theta = 0 \tag{11}$$

Taking the trace of equation (2) and using equations (3) and (10), one obtains the Raychaudhuri equation:

$$\frac{d\theta}{d\tau} + \frac{\dot{a}}{a}\theta + \frac{1}{3}\theta^2 + \sigma^{ij}\sigma_{ij} - 2\omega^2 = -4\pi G a^2 \bar{\rho}\delta , \tag{12}$$

where $\omega^2 \equiv \omega^i\omega_i$. Similarly, taking the antisymmetric and traceless symmetric parts of equation (2) gives respectively

$$\frac{d\omega^i}{d\tau} + \frac{\dot{a}}{a}\omega^i + \frac{2}{3}\theta\,\omega^i - \sigma^i{}_j\,\omega^j = 0 \tag{13}$$

and

$$\frac{d\sigma_{ij}}{d\tau} + \frac{\dot{a}}{a}\sigma_{ij} + \frac{2}{3}\theta\,\sigma_{ij} + \sigma_{ik}\sigma^k{}_j + \omega_i\omega_j - \frac{1}{3}\delta_{ij}\left(\sigma^{kl}\sigma_{kl} + \omega^2\right) = -E_{ij} , \tag{14}$$

where $E_{ij} \equiv \nabla_i\nabla_j\phi - (1/3)\,\delta_{ij}\,\nabla^2\phi$ is the gravitational tidal field.

In keeping with the spirit of Lagrangian fluid dynamics, we would like an evolution equation for E_{ij}. From equations (1) and (3), Bertschinger & Hamilton (1994) derived

$$\frac{dE_{ij}}{d\tau} + \frac{\dot{a}}{a}\,E_{ij} - \nabla_k\,\epsilon^{kl}{}_{(i}H_{j)l} + \theta E_{ij} + \delta_{ij}\,\sigma^{kl}E_{kl} - 3\sigma^k{}_{(i}E_{j)k} - \omega^k{}_{(i}E_{j)k} = -4\pi G a^2\rho\,\sigma_{ij} . \tag{15}$$

Parentheses around a pair of subscripts indicates symmetrization, e.g., $\sigma^k{}_{(i}E_{j)k} = (\sigma^k{}_iE_{jk} + \sigma^k{}_jE_{ik})/2$. The new quantity H_{ij} is the Newtonian limit of the magnetic part of the Weyl tensor in the fluid frame. The definition and discussion of this term will be deferred until the next section.

Equations (11) to (15) form a hierarchy of Lagrangian fluid equations. It is an incomplete set because we have not stated the evolution equation for H_{ij}. In order to arrive

at a local set, we must eliminate the gradient term in equation (15), either by finding an approximation for $-\nabla_k \, \epsilon^{kl}{}_{(i} H_{j)l}$ or by truncating the hierarchy in a way that eliminates our need to determine it.

The ZA eliminates the need to calculate H_{ij} by approximating the evolution of the gravity field — equation (9) relates $\vec{\nabla}\phi$ to $\vec{v}$. As a result, the tidal tensor in the ZA follows from the shear:

$$E_{ij} = -\frac{4\pi G a \bar{\rho}}{H f}\sigma_{ij} = -\frac{3\Omega_0 H_0^2}{2\dot{a}\,f}\sigma_{ij} \; . \tag{16}$$

Furthermore, the divergence of the gravity field is given in the ZA by the velocity expansion scalar θ instead of the density fluctuation. Thus, the ZA is equivalent to solving the local evolution equations

$$\frac{d\theta}{d\tau} + \frac{\dot{a}}{a}\,\theta + \frac{1}{3}\,\theta^2 + \sigma^{ij}\sigma_{ij} - 2\omega^2 = \frac{4\pi G a \bar{\rho}}{H f}\theta \; , \tag{17}$$

$$\frac{d\sigma_{ij}}{d\tau} + \frac{\dot{a}}{a}\,\sigma_{ij} + \frac{2}{3}\,\theta\,\sigma_{ij} + \sigma_{ik}\sigma^k{}_j + \omega_i\omega_j - \frac{1}{3}\,\delta_{ij}\left(\sigma^{kl}\sigma_{kl} + \omega^2\right) = \frac{4\pi G a \bar{\rho}}{H f}\sigma_{ij} \; . \tag{18}$$

Together with equations (11) and (13), these give a closed set of equations for the evolution of quantities for a single mass element with no spatial gradients. This is what we mean by locality. Note that we have assumed the irrotational flow initial condition and so $\omega_{ij} = 0$ from equation (13) at all times before trajectories intersect. Equation (18) can be written also as an evolution equation for E_{ij} by making use of equation (16) (Kofman & Pogosyan 1995). But it is clear that in terms of obtaining a closed set of local equations, it is sufficient to stop at the level of the shear equation (18).

Hence, we have shown that the ZA is a local approximation based on truncating the set of Lagrangian fluid equations at the shear evolution equation by setting E_{ij} proportional to σ_{ij} and by approximating the gravitational source term in the Raychaudhuri equation. It is then very natural to ask whether we can go further, by using the exact Raychaudhuri equation and by truncating the system of equations at the tidal evolution equation with a different approximation from the ZA.

There is a simple argument for why we should expect to be able to improve on the ZA. It is well known that the ZA gives incorrect results for spherical infall. For spherical infall, the velocity and gravity fields are isotropic around a point, so that $\sigma_{ij} = E_{ij} = 0$ at that point. Yet, the ZA overestimates the collapse time for a uniform spherical tophat. The reason for this is that the ZA does not obey the Poisson equation, so the right-hand side of equation (17) is not exact. We can at least correct this term. We have tested this approximation — using equation (12) in place of equation (17), and using equation (18) for the shear evolution — and found that it works poorly aside from spherical flow. Thus, we seek improved approximations based on a more accurate treatment of the tidal tensor.

3. Two Local Approximations Based on the Tidal Evolution Equation

As remarked in the last section, the hierarchy of Lagrangian fluid equations can be truncated at the tidal evolution equation, provided that we approximate, or eliminate, the H_{ij} term (and possibly other terms also). If possible, we would like to find local approximations that retain the successes of the Zel'dovich approximation. These include giving the correct results in linear perturbation theory and giving the exact solution for plane-parallel flows. Ideally, we would also like to improve on the Zel'dovich approximation by giving exact results for spherical and/or cylindrical flows. We use these criteria in seeking improved approximations.

Let's look at the magnetic part of the Weyl tensor more closely. The definition is given in Bertschinger & Hamilton (1994):

$$H_{ij} \equiv -\frac{1}{2}\nabla_{(i}H_{j)} - 2\,v_k\,\epsilon^{kl}{}_{(i}E_{j)l} \tag{19}$$

where H_i satisfies:

$$\vec{\nabla}\times\vec{H} = -16\pi Ga^2\,\vec{f}_\perp\,, \quad \vec{\nabla}\cdot\vec{H} = 0\,. \tag{20}$$

Here $\vec{f}_\perp$ is the transverse part of the mass current, defined as follows:

$$\vec{f}_\perp \equiv f - f_\parallel = \rho\vec{v} - f_\parallel\,, \quad \vec{f}_\parallel = -\frac{1}{4\pi Ga^3}\vec{\nabla}\left(\frac{\partial\,a\phi}{\partial\tau}\right)\,. \tag{21}$$

Using these definitions, we can rewrite equation (15) as follows:

$$\frac{dE_{ij}}{d\tau} + \frac{\dot{a}}{a}E_{ij} + M_{ij} = -4\pi Ga^2\rho\sigma_{ij}\,, \tag{22}$$

where

$$\begin{aligned}
M_{ij} &\equiv -\nabla_k\,\epsilon^{kl}{}_{(i}H_{j)l} + \theta E_{ij} + \delta_{ij}\,\sigma^{kl}E_{kl} - 3\sigma^k{}_{(i}E_{j)k} - \omega^k{}_{(i}E_{j)k} \\
&= -4\pi Ga^2\rho\nabla_{(i}v_{j)} - \frac{1}{a}\frac{d}{d\tau}(\nabla_i\nabla_j a\phi) \\
&= -4\pi Ga^2\nabla_{(i}f_{\perp j)} - v_k\nabla^k\nabla_i\nabla_j\phi + v_{(i}\nabla_{j)}\nabla^2\phi\,.
\end{aligned} \tag{23}$$

Let us first consider plane-parallel flows, for which the ZA is exact. The velocity and gravity gradient tensors may be written

$$\nabla_i v_j = \theta\,\mathrm{diag}(0,0,1)\,, \quad \nabla_i\nabla_j\phi = \nabla^2\phi\,\mathrm{diag}(0,0,1)\,, \tag{24}$$

where diag() denotes the elements of the diagonalized tensor. Evaluating M_{ij} using equations (23), we find that the curl H_{jl} term as well as the sum of terms proportional to

the tidal tensor vanish identically. The individual tidal terms do not vanish. This result suggests two different closure schemes for the tidal evolution equation (22). The first one is to discard $\nabla_k \epsilon^{kl}{}_{(i} H_{j)l}$. The second is to discard the complete tensor M_{ij}. If some of the tidal terms of M_{ij} were retained, the resulting approximation would not be exact for one-dimensional flows, hence would not improve on the Zel'dovich approximation.

The first choice, setting $H_{ij} = 0$ in equation (15), was proposed by Bertschinger & Jain (1994):

$$\frac{dE_{ij}}{d\tau} + \frac{\dot{a}}{a} E_{ij} + \theta E_{ij} + \delta_{ij} \sigma^{kl} E_{kl} - 3\sigma^k{}_{(i} E_{j)k} - \omega^k{}_{(i} E_{j)k} = -4\pi Ga^2 \rho\, \sigma_{ij} \; . \tag{25}$$

We shall call this the non-magnetic approximation (NMA). Combined with equations (11)–(14), it provides a closed set of local evolution equations. The NMA was inspired, in part, by the remark of Ellis (1971) that the magnetic part of the Weyl tensor has no Newtonian counterpart. However, it leads to unusual behavior, implying that cold dust fluid elements generically collapse to spindles (Bertschinger & Jain 1994). Also, Bertschinger & Hamilton (1994) were able to derive equation (15) with H_{ij} defined using equations (19)–(21) from Newton's laws in an expanding universe, as well as constraint and evolution equations for H_{ij} itself (the latter using post-Newtonian corrections), from which we now know that H_{ij} is not identically zero in the Newtonian limit, aside from some special cases of high symmetry.

Thus, we are motivated to try the second approximation, setting $M_{ij} = 0$ in equation (22):

$$\frac{dE_{ij}}{d\tau} + \frac{\dot{a}}{a}E_{ij} = -4\pi Ga^2 \rho\sigma_{ij} \; . \tag{26}$$

Equation (26) and equations (11)–(14) form our new set of closed local equations. We shall call this the Local Tidal Approximation (LTA) to distinguish it from equation (25), the non-magnetic approximation.

The LTA, like the ZA, is exact for plane-parallel flows prior to the intersection of orbits. What about spherically and cylindrically symmetric flows, for which the ZA is not exact? For the LTA, we use equations (23) to evaluate M_{ij} for flows that are spherically symmetrical around the fluid element under consideration. As long as the gravity gradient is finite at the origin (a condition that holds for any continuous finite-density mass distribution), this restriction implies that all three eigenvalues of $\nabla_i \nabla_j \phi$ are equal, so $E_{ij} = 0$ identically (similarly $\sigma_{ij} = 0$). Equations (25) and (26) are satisfied trivially. Thus, the LTA is exact for spherical mass elements. So is the NMA.

Next we consider a non-singular fluid element on the symmetry axis of a cylindrically symmetric flow. By this we mean that two eigenvalues of $\nabla_i \nabla_j \phi$ are equal and the third

one vanishes and similarly for $\nabla_i v_j$. In this case we have

$$\nabla_i v_j = \frac{1}{2}\,\theta\,\text{diag}(1,1,0)\ , \quad \nabla_i\nabla_j\phi = \frac{1}{2}\,\nabla^2\phi\,\text{diag}(1,1,0)\ . \tag{27}$$

Using this, it is easy to show that the sum of tidal terms in the first form of equation (23) do not vanish, while, with equations (3) and (11), the second form for M_{ij} leads to $M_{ij} = 0$. Thus, the LTA is also exact for cylindrical flows, while the NMA is not. Bertschinger & Jain (1994) erred in saying that the NMA was exact for cylindrical flows.

One can generalize these results to show from the second form of equation (23) that $M_{ij} = 0$ for any flow for which $(\nabla^2\phi)^{-1}\nabla_i\nabla_j\phi$ equals $\theta^{-1}\nabla_{(i}v_{j)}$ and is a constant tensor. These conditions are equivalent to saying that the orientation and axis ratios of the gravitational and velocity equipotentials are constant for the mass element under consideration. Thus, the LTA is exact for flows with equipotentials of constant shape. Although this condition does not always hold, it is valid for the growing mode in the linear regime and it includes spherically and cylindrically symmetric flows as well as plane-parallel flows. Moreover, the gravitational potential contours are more nearly spherical than the density contours around a peak, so their shape would be expected to change relatively slowly with time, suggesting that the LTA may be a good approximation in general.

In the linear regime, the LTA, NMA, and ZA all agree. It is already clear that they must differ in second-order perturbation theory; the Appendix presents the calculation of $\nabla_k\,\epsilon^{kl}\,_{(i}H_{j)l}$ and M_{ij}. However, it is more important to see how these various approximations behave as collapse is approached. We know already that generic initial conditions lead to collapse along one dimension (pancake) with the ZA (from Bertschinger & Jain 1994) while the NMA leads to collapse along two dimensions (spindle). What about the LTA? How accurate is the LTA for asymmetrical initial conditions? Before answering these questions we first examine the relative sizes of the terms in equation (22) for an overdense homogeneous ellipsoid in an expanding universe.

4.   Collapse of a Homogeneous Ellipsoid

We summarize here the equations of motion for an irrotational homogeneous ellipsoid embedded in an expanding universe. The various interesting quantities in the tidal evolution equation are then calculated for the collapse of a particular ellipsoid.

We consider an irrotational homogeneous ellipsoid with proper axis lengths R_1, R_2, and R_3 embedded in a Friedmann-Robertson-Walker background. The equations of motion

are (Icke 1973; White & Silk 1979):

$$\frac{d^2 R_i}{dt^2} = -2\pi G R_i \left[\frac{2}{3}\rho_b + \alpha_i(\rho_e - \rho_b)\right] \ , \tag{28}$$

where t is the proper time $(dt = a d\tau)$ and α_i is defined by

$$\alpha_i = R_1 R_2 R_3 \int_0^\infty \frac{ds}{(R_i{}^2 + s)\sqrt{(R_1{}^2 + s)(R_2{}^2 + s)(R_3{}^2 + s)}} \ . \tag{29}$$

Here ρ_e is the total density within the ellipsoid while ρ_b is the density of the expanding universe surrounding the ellipsoid. They are related to the mean and perturbed densities used previously by $\rho_b = \bar\rho$ and $\rho_e = \bar\rho(1 + \delta)$. We evaluate them from the evolution of the axis lengths and the background expansion scale factor:

$$\rho_e R_1 R_2 R_3 = \rho_{eo} \ , \quad \rho_b a^3 = \rho_{bo} \ , \tag{30}$$

where ρ_{eo} and ρ_{bo} are constants. Note that $\alpha_1 + \alpha_2 + \alpha_3 = 2$ and we assume $\Omega_0 = 1$. Note also that since equation (28) is second order, there are in general two independent modes. We choose growing mode initial conditions. For small a the first order solution or, equivalently, the ZA result, is

$$R_i(t) = a(t)X_i \left(1 - \frac{1}{2}\alpha_{i0}\delta_0 a\right) \tag{31}$$

where the X_i's give the initial axis ratios, α_{i0} gives the initial ellipsoid parameter, and δ_0 gives the linear amplitude of the density perturbation. We set $\delta_0 = 1$ for overdense ellipsoids without loss of generality.

Equation (30) implies that the total mass, including the mass inside the ellipsoid as well as outside, is actually not conserved even though the mass inside the ellipsoid is. Hence equation (28) can only be an approximation to the true evolution of an initially homogeneous ellipsoid. In general, one expects that such an ellipsoid would cause the density of its immediate surroundings to deviate from the cosmic mean. Tidal fields from this perturbed external material should then induce departure from homogeneity in the ellipsoid. Based on results from an N-body simulation (S. D. M. White 1993, private communication), we assume that it is a good approximation to ignore departures from homogeneity inside and outside the ellipsoid when calculating the evolution of the axis ratios.

It is noteworthy that equation (28) is exact if $\rho_b = 0$, i.e., for a homogeneous ellipsoid in a vacuum. Later in this section we will test our approximations using the exact solution in this case.

The peculiar velocity field inside the homogeneous ellipsoid is described by:

$$v_i = \left(\frac{\dot{R}_i}{R_i} - \frac{\dot{a}}{a} \right) x_i \qquad (32)$$

and the gravitational potential within the ellipsoid is:

$$\phi = \pi G a^2 (\rho_e - \rho_b) \sum_i \alpha_i x_i^2 \ . \qquad (33)$$

(The x_i are comoving coordinates and dots denote conformal time derivatives.) Quantities like the expansion, shear, and tidal field can be immediately read off from these expressions:

$$\theta = \sum_i \frac{\dot{R}_i}{R_i} - 3\frac{\dot{a}}{a} \ , \qquad (34)$$

$$\sigma_{ij} = \mathrm{diag} \left(\frac{\dot{R}_i}{R_i} - \frac{1}{3} \sum_k \frac{\dot{R}_k}{R_k} \right) \ , \qquad (35)$$

$$E_{ij} = 2\pi G a^2 (\rho_e - \rho_b) \, \mathrm{diag} \left(\alpha_i - \frac{2}{3} \right) \ . \qquad (36)$$

The tensor M_{ij} defined in equation (23) is given for the homogeneous ellipsoid by

$$M_{ij} = 2\pi G a^2 \rho_e \, \mathrm{diag} \left[-2\sigma_{ij} + \left(\alpha_i - \frac{2}{3} \right) \theta - \frac{\delta}{1+\delta} \dot{\alpha}_i \right] \ . \qquad (37)$$

Using the time evolution of R_i given by equation (28), the evolution of the various quantities above can be calculated. In particular, we are interested in the relative magnitude of various terms in the tidal evolution equations (15) and (22). We integrated equations (28) and (29) numerically starting from equation (31) at $a = 10^{-8}$ with axis ratios $1 : 1.25 : 1.5$. From the axis lengths R_i and their time derivatives, using equations (34)–(36) we calculated the velocity and gravity gradient terms inside the ellipsoid. From these we then calculated the evolution of $-\nabla_k \, \epsilon^{kl}_{\ \ (i} H_{j)l}$, M_{ij}, and $4\pi G a^2 \rho \sigma_{ij}$ inside the ellipsoid. Note that in this test we do not integrate the tidal evolution equation itself; rather, we evaluate the terms in it assuming that the system evolves according to the homogeneous ellipsoid solution. Although, as we noted above, this solution is not exact, we are being self-consistent by evaluating the various tensor quantities using equations (34)–(37), which assume spatial homogeneity inside the ellipsoid.

Figure 1 shows the results of this calculation. The magnitudes of $-\nabla_k \, \epsilon^{kl}_{\ \ (i} H_{j)l}$ and M_{ij} are divided by the magnitude of $4\pi G a^2 \rho \sigma_{ij}$, where by the magnitude of a matrix we mean the square root of the trace of its square. We see that $-\nabla_k \, \epsilon^{kl}_{\ \ (i} H_{j)l}$ and M_{ij} are both
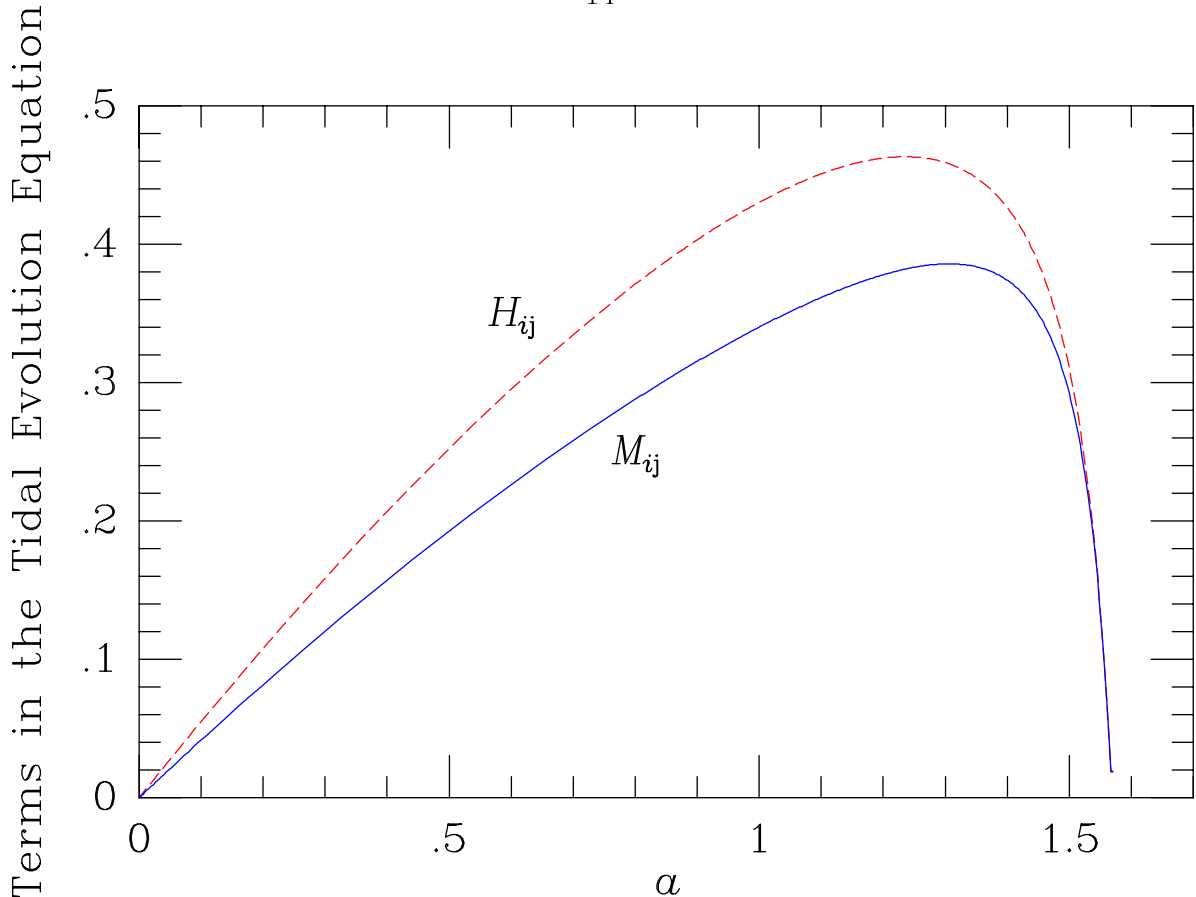
Fig. 1.— Evolution of the magnitudes of $-\nabla_k \, \epsilon^{kl}{}_{(i}H_{j)l}$ (dashed line) and M_{ij} (solid line) divided by the magnitude of $4\pi G a^2 \rho \sigma_{ij}$, evaluated for a homogeneous ellipsoid with initial axis ratios $1 : 1.25 : 1.5$ embedded in an expanding universe. The magnitude of a matrix is defined here as the square root of sum of squares of eigenvalues.

small compared to $4\pi G a^2 \rho \sigma_{ij}$ at both early and late times, but not intermediate times (near maximum expansion). Interestingly, the magnetic term and M_{ij} have similar magnitude throughout the collapse process.

We can easily understand why $4\pi G a^2 \rho \sigma_{ij}$ is much bigger than both $-\nabla_k \, \epsilon^{kl}{}_{(i}H_{j)l}$ and M_{ij} at early times using perturbation theory. The shear is first order. The last form of equations (23) is the best place to see that M_{ij} is second order: $f_{\perp i}$ is second order because, to first order, $f_i = \bar{\rho} v_i$ is longitudinal (we assume irrotational initial conditions). The other contributions to M_{ij} are obviously second order. From the first form of equation (23), we conclude also that $-\nabla_k \, \epsilon^{kl}{}_{(i}H_{j)l}$ is second order. Expressions for these two tensors in second order perturbation theory are given in the Appendix. They are both nonzero in general.

The behavior of these quantities close to the moment of pancake collapse can also

be estimated analytically. Suppose that the third axis collapses while the other two axes still have finite lengths. The term $4\pi Ga^2\rho\sigma_{ij}$ diverges at the moment of pancake collapse because ρ diverges and so does σ_{ij}, owing to the $\dot{R}_3/R_3$ term in equation (35). For the behavior of $-\nabla_k\,\epsilon^{kl}{}_{(i}H_{j)l}$ and M_{ij} approaching collapse, we need to understand the behavior of the α_i's.

It follows from equation (29) that α_1 and α_2 vanish in the limit of vanishing R_3 for finite R_1 and R_2, because the integral is finite while the factor of R_3 in front vanishes. Note also, by definition, the three α_i's always add up to 2. Hence $\alpha_3 = 2$ at collapse. Moreover, it can be verified using equation (29) that the $\dot{\alpha}_i$'s are finite at the moment of collapse, assuming the $\dot{R}_i$'s are finite. It can then be shown using equations (34)–(37) that the particular combination of α_i's conspires to render both $M_{ij}/4\pi Ga^2\rho$ and $-\nabla_k\,\epsilon^{kl}{}_{(i}H_{j)l}/4\pi Ga^2\rho$ finite. Hence at the moment of pancake collapse, $-\nabla_k\,\epsilon^{kl}{}_{(i}H_{j)l}$ and M_{ij} are indeed much smaller than $4\pi Ga^2\rho\sigma_{ij}$.

The fact that $-\nabla_k\,\epsilon^{kl}{}_{(i}H_{j)l}$ and M_{ij} are both small compared to $4\pi Ga^2\rho\sigma_{ij}$ at early times and at the moment of pancake collapse suggests that the NMA and LTA might both be good approximations. However, Figure 1 shows that these terms are not negligible throughout the collapse process. Hence there is no guarantee that either approximation can reproduce the correct features of the collapse process. In particular, we do not know from these results whether the NMA or LTA would produce pancake collapse given the initial conditions we have chosen. We also do not know which approximation will be more accurate for generic initial conditions, although Figure 1 suggests that it may be better to neglect M_{ij} than H_{ij}.

5.   Pancakes Versus Spindles

The oblate and prolate configurations are distinguished by the signature of the eigenvalues of E_{ij} and σ_{ij}. For the collapsing oblate (pancake) configuration, the eigenvalues of E_{ij} have the signature $(-,-,+)$ and those of σ_{ij} have $(+,+,-)$. For the collapsing prolate (spindle) configuration, E_{ij} has eigenvalues with signature $(-,+,+)$ and σ_{ij} has $(+,-,-)$. One way to see why this is true is by inspecting equations (35) and (36). For the pancake configuration, one can use the fact that α_3 is close to 2 (supposing collapse occurs in the third direction) while α_1 and α_2 almost vanish. For the spindle configuration, suppose that collapse occurs for the second and third direction and suppose for simplicity that they collapse at the same rate. Then from equation (29), one can show that close to the spindle configuration, $\alpha_3 \simeq \alpha_2 \simeq 1$ and $\alpha_1 \simeq 0$. Using this and equations (35) and (36), it is possible to obtain the signature for the eigenvalues of E_{ij} and σ_{ij}. Note also that it is

sufficient to consider only the divergent parts of E_{ij} and σ_{ij} to get the right signatures.

Consider equation (25). This is the tidal evolution equation of the NMA, which ignores the magnetic part of the Weyl tensor. First of all, the term proportional to $\dot{a}/a$ always tends to decrease E_{ij}, encouraging spherical collapse. But by the time the motion of the object under consideration breaks away from the expansion of the universe, this term becomes unimportant. Suppose now that the object is close to the pancake configuration with E_{ij} having signature $(-,-,+)$ and σ_{ij} having $(+,+,-)$. Then it can be seen that all the terms favor pancake collapse (or favor neither pancakes nor spindles) except the shear-tide coupling terms $\delta_{ij}\sigma^{kl}E_{kl} - 3\sigma^{k}{}_{(i}E_{j)k}$. The net sign of these two terms is such that the growth of E_{ij} towards the pancake signature is suppressed. Suppose on the other hand that the object is close to the spindle configuration with E_{ij} and σ_{ij} having signatures $(-,+,+)$ and $(+,-,-)$ respectively. Then all the terms, including the shear-tide couplings, encourage the growth of tide towards the spindle signature. In other words, the NMA on the whole favors collapse toward the prolate or spindle configuration.

Consider, on the other hand, the exact tidal evolution equation (22). For an object with a very short third axis compared to the other two, we expect α_3 to be slightly less than but close to 2 and α_1 and α_2 to be small and positive. Substituting this into equation (37) and looking only at the most divergent terms, one can verify that M_{ij} has signature $(-,-,+)$ close to the pancake configuration. Using similar arguments, it can be deduced that M_{ij} has signature $(-,+,+)$ close to the spindle configuration. Hence, M_{ij} has the same signature as E_{ij} close to collapse, whether it be pancake or spindle; therefore it stabilizes collapse just like the Hubble damping term proportional to $\dot{a}/a$. Hence ignoring M_{ij}, which is the LTA, does not favor spindles over pancakes. This is very different from the NMA.

Equation (23) tells us that M_{ij} contains both $-\nabla_k \epsilon^{kl}{}_{(i}H_{j)l}$ and the shear-tide coupling terms. We can now see what is wrong with the NMA — for the spindle configuration, $-\nabla_k \epsilon^{kl}{}_{(i}H_{j)l}$ has a signature that is opposite to the shear-tide coupling terms, and it is large enough to reverse the spindle-enhancing effect of the latter. As a result, M_{ij} as a whole, which includes the sum of these terms, plays no favorites.

Numerical integration bears out this analysis. We tested the LTA and NMA by integrating the sets of local Lagrangian fluid equations which are obtained by ignoring the relevant terms in the tidal evolution equation: equations (11), (12), (14), and either (25) or (26). The tensor equations were diagonalized along principal axes. Initial conditions were chosen using equations (31) and (34)–(36) so as to correspond to the homogeneous ellipsoid model with initial axis ratios $1 : 1.25 : 1.5$. Given the numerical solution for $\theta(\tau)$ and $\sigma_{ij}(\tau)$, we then predicted the evolution of the homogeneous ellipsoid axis lengths by solving equations (34)–(35) for $\dot{R}_i/R_i$ and numerically integrating it to get $R_i(\tau)$. For comparison,

we also computed the prediction of the ZA for the axis evolution given the same initial
conditions. We obtained the same results for the ZA by integrating the local Lagrangian
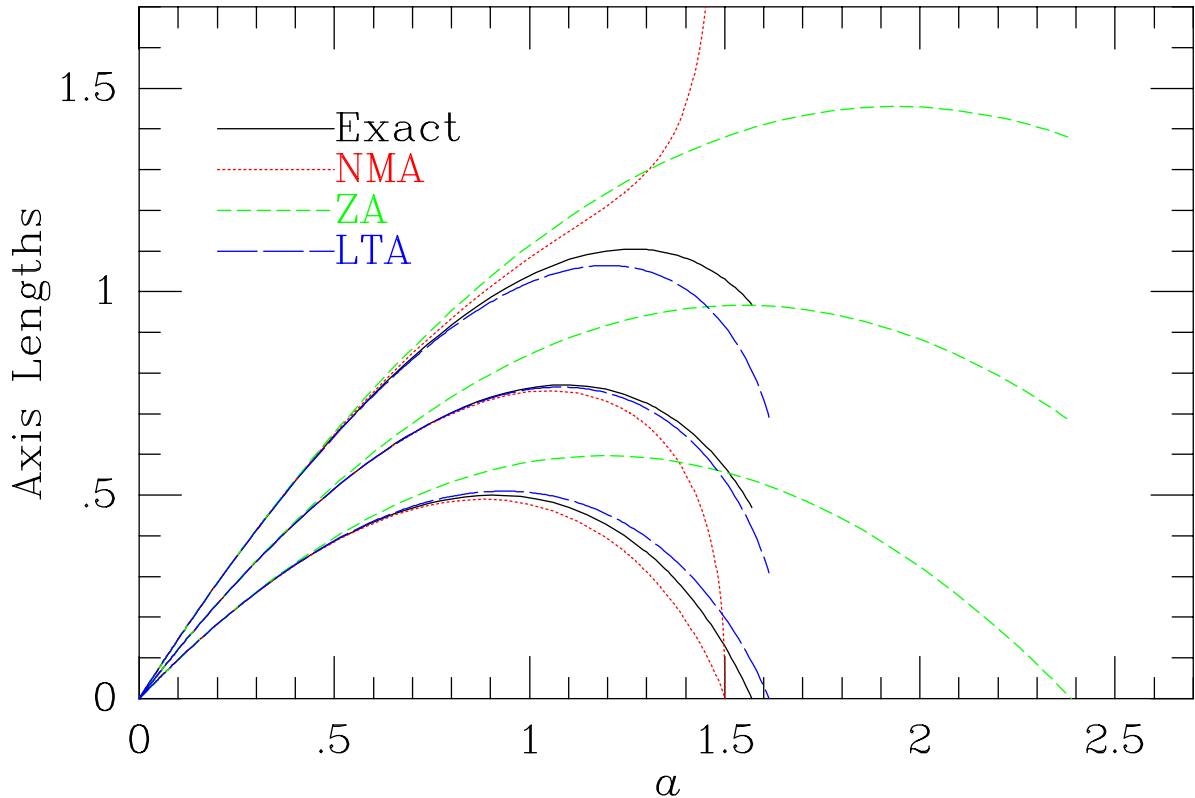fluid equations (17) and (18) as we did from equation (31).

Fig. 2.— The evolution of axis lengths for a homogeneous ellipsoid embedded in an expanding
universe. The initial axis ratios are 1 : 1.25 : 1.5. The "exact" solution (ignoring development
of inhomogeneity, solid curve) is compared with the ZA (short dashed curve) and two
local approximations: the local tidal approximation (LTA, long dashed curve) and the non-
magnetic approximation of Bertschinger & Jain (NMA, dotted curve).

Figure 2 compares the local approximations (ZA, LTA, NMA) for the evolution of
the axis lengths with each other and with the solution given by integrating equations
(28). Both the ZA and LTA reproduce the qualitative features of pancake collapse. As
we have already noted, the NMA predicts collapse to a spindle instead of pancake. For
these initial conditions, at least, the LTA is even more accurate than the ZA. The LTA
overestimates the expansion factor at collapse by only 3%, compared with 52% for the ZA.
The LTA appears to rectify one of the well-known problems with the ZA, namely the fact

that it underestimates the rapidity of collapse for non-planar perturbations. This result is consistent with our observation in §3 that the LTA is exact for spherical and cylindrical symmetry.
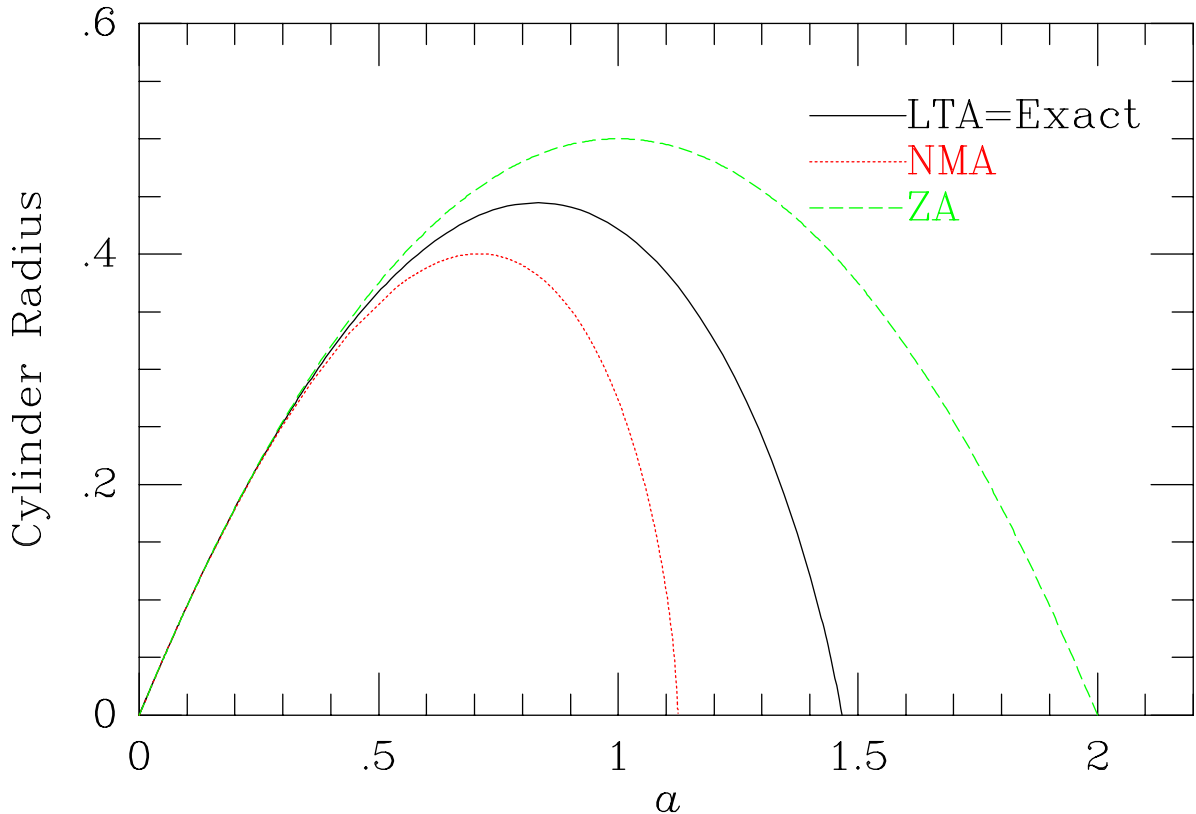

Fig. 3.— The evolution of the radius of a cylindrical perturbation in an expanding universe, corresponding to a homogeneous ellipsoid with axes $R : R : \infty$ (a cylinder). The exact solution (solid curve) is compared with the ZA (short dashed curve) and the NMA (dotted curve). The LTA is exact for this case.

It is also useful to compare the local approximations with the exact solution for cylindrically symmetric perturbations. Consider a homogeneous overdense cylinder in an Einstein-de Sitter universe, with radius $R(t)$. The equation of motion is given by Fillmore & Goldreich (1984). It can be written in a form corresponding to equation (28):

$$\frac{d^2 R}{dt^2} = -2\pi G R \left[\frac{2}{3} \rho_b + (\rho_c - \rho_b) \right] , \tag{38}$$

where ρ_c is the density inside the cylinder. In fact, this is identical to equation (28) for a homogeneous ellipsoid with axis ratios $R : R : \infty$, for which $\alpha_1 = \alpha_2 = 1$, $\alpha_3 = 0$.

We repeated the comparison of local approximations with the exact solution given by integrating equation (38). The results are shown in Figure 3. The LTA is exact, while the NMA underestimates the expansion factor at collapse (by 23%) and the ZA overestimates it (by 36%).
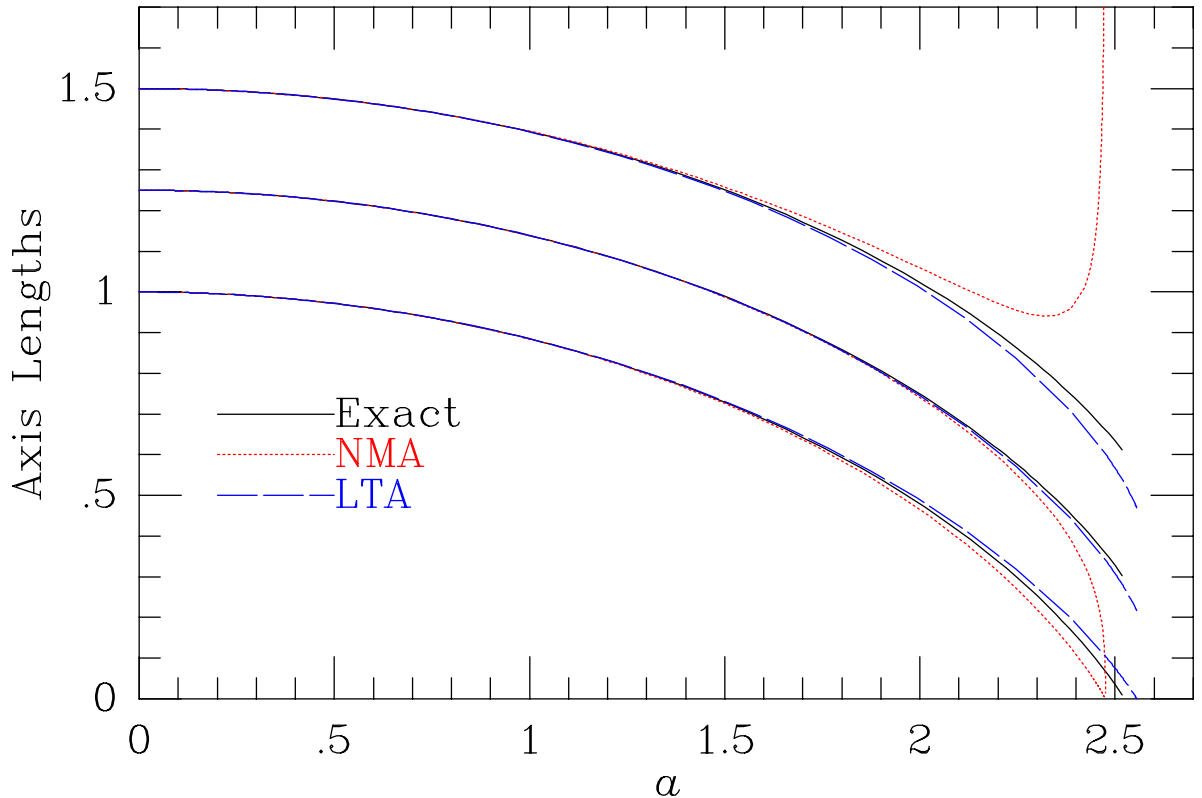

Fig. 4.— The evolution of axis lengths for a homogeneous ellipsoid embedded in empty space. The initial axis ratios are $1 : 1.25 : 1.5$. The exact solution (solid curve) is compared with the predictions of LTA (long dashed curve) and NMA (dotted curve).

An exact solution also exists for a homogeneous ellipsoid in a vacuum (non-expanding) background (Lin, Mestel, & Shu 1965). It is easy to modify the NMA and LTA equations for this case, by setting $a = 1$ and $\rho_b = \bar{\rho} = 0$. We did not integrate the non-cosmological analog of the ZA. As for Figure 2, we set the initial axis ratios to be $1 : 1.25 : 1.5$, although in this case we set the initial velocity field to zero. Figure 4 shows the results. Once again we see that the LTA is rather accurate for generic initial conditions (the collapse time here is 1.5% too large) and leads to pancake collapse, while the NMA incorrectly predicts spindle collapse.

To compare the three local approximations (ZA, NMA, LTA) with more general initial conditions, we follow the notations of Bertschinger & Jain (1994) and write traceless symmetric tensors in terms of a magnitude and an angle:

$$\sigma_{ij} = \frac{2}{3}\, \sigma\, Q_{ij}(\alpha)\ , \quad E_{ij} = \frac{8\pi}{3}\, G\bar{\rho}a^2\, \epsilon\, (1+\delta)\, Q_{ij}(\beta)\ . \tag{39}$$

We have introduced new scalars $\sigma \le 0$, $\epsilon \ge 0$, α and β $(0 \le \alpha, \beta \le \pi)$, and a one-parameter traceless quadrupole matrix

$$Q_{ij}(\alpha) \equiv \mathrm{diag}\left[\cos\left(\frac{\alpha+2\pi}{3}\right),\, \cos\left(\frac{\alpha-2\pi}{3}\right),\, \cos\left(\frac{\alpha}{3}\right)\right]\ . \tag{40}$$

With this parametrization, oblate configurations have $\cos\alpha > 0$ while prolate configurations have $\cos\alpha < 0$. Of course, the shape of a perturbation can change with time. The equations of motion for σ, ϵ, α, and β for the NMA are given by Bertschinger & Jain. For the LTA, their equations (13) and (14) are changed to become

$$\frac{d\epsilon}{d\tau} - \theta\epsilon = -\sigma\cos\left(\frac{\alpha-\beta}{3}\right)\ , \tag{41}$$

$$\frac{d\beta}{d\tau} = -\frac{3\sigma}{\epsilon}\sin\left(\frac{\alpha-\beta}{3}\right)\ . \tag{42}$$

One quantity of interest for general initial conditions is the expansion factor at collapse, i.e., the linear overdensity when a given mass element collapses. Following Bertschinger & Jain (1994), we parametrize the initial conditions by ϵ_0 and α_0, which are related to the values of ϵ and α in linear theory through $\epsilon = a\epsilon_0$ and $\alpha = \alpha_0$. Because initially underdense perturbations can collapse if the shear is sufficiently strong, we treat both initially overdense and underdense perturbations by specifying $\delta_0 = \pm 1$, respectively (δ_0 being related to δ in linear theory by $\delta = a\delta_0$). The expansion factor at collapse, a_c, is determined by integrating the local evolution equations for the LTA and NMA. For the ZA, it is simpler to use equations (4) and (8), noting that collapse occurs when the determinant of $\partial x^i/\partial q_j$ vanishes. With our parametrization of the initial velocity and gravity gradient tensors, it follows that

$$a_c = \frac{3}{\delta_0 + 2\epsilon_0\cos(\alpha_0/3)}\quad (\mathrm{ZA})\ . \tag{43}$$

The collapse expansion factor a_c is defined to be the absolute value of the linear overdensity when a given mass element collapses to infinite density. For example, an overdense spherical perturbation collapses when $a_c = 1.686$, while a cylindrical perturbation collapses when $a_c = 1.466$ and a plane-parallel perturbation collapses when $a_c = 1$. Although there exists no exact solution for arbitrary initial conditions, it is informative to compare all three methods. Based on our previous results we expect the LTA to be accurate to a few percent.

We plot contours of constant collapse time for different initial tidal parameters ϵ_0 and α_0 for the three local approximations in Figure 5. In each part, the left panel gives results for overdense perturbations while the right panel is for initially underdense perturbations. Figure 5b presents the same results as Figures 1 and 2 of Bertschinger & Jain (1994). We see that the LTA and ZA are qualitatively similar, although the ZA overestimates the collapse time for overdense configurations with small tide (near the center of the figures). According to the ZA, $a_c = 3$ for spherical perturbations while the exact value is $\frac{5}{3}(2/3\pi)^{2/3} = 1.68647\ldots$ Both the ZA and LTA indicate more rapid collapse for initially oblate configurations. As noted by Bertschinger & Jain, initially prolate configurations collapse faster in the NMA because according to its incorrect dynamics initially oblate configurations must change shape before collapsing to a spindle.

Bertschinger & Jain (1994) also noted that shear can lead to collapse of underdense perturbations. From Figure 5, we see that that the size of the non-collapsing region in parameter space (in the middle of the right-hand panels) is largest for the NMA and smallest for the ZA, indicating that the NMA underestimates the fraction of initial underdense perturbations that can collapse, while the ZA overestimates it. Using the probability distribution of ϵ_0 and α_0 derived by Bertschinger & Jain for a Gaussian random field, we find that the probability that a randomly chosen mass element will collapse is 0.780 for NMA, 0.888 for LTA, and 0.920 for ZA. Thus, taking the LTA as the most accurate, approximately 78% ($= 2 \times 0.888 - 1$) of the underdense perturbations (and 100% of the overdense ones) will collapse. This estimate neglects the crossing of mass elements, which increases the likelihood of collapse by increasing the density. Indeed, we expect every mass element collapses eventually in a perturbed self-gravitating cold dust medium.

6.   Conclusion

In this paper, we have discussed three different local approximations for gravitational collapse of perturbations in an expanding universe: the Zel'dovich approximation (ZA), the non-magnetic approximation (NMA) of Bertschinger & Jain (1994), and a new local tidal approximation (LTA) introduced here. Conventionally, the ZA is presented as a mapping of Lagrangian to Eulerian positions. However, we showed that it can also be regarded as a certain truncation of the set of Lagrangian fluid equations for the density, velocity gradient, and tide following a fluid element of cold dust. With the ZA, the gravity gradient is explicitly proportional to the velocity gradient, resulting in modifications to the Raychaudhuri and shear evolution equations. The tidal evolution equation need not be integrated in the ZA because the gravity field acting on a mass element is given by a simple

extrapolation of initial conditions. The other two approximations we discuss extend the ZA by integrating the exact Raychaudhuri and shear evolution equations, with approximations made only to the tidal evolution equation.

All three local approximations are exact for plane-parallel perturbations. However, the behavior for other shapes of perturbations shows significant differences in behavior. The ZA is only approximate for non-plane-parallel distributions. The NMA is exact for spherical perturbations but not cylindrical ones. The LTA is exact for spherical and cylindrical perturbations and, more generally, for any growing-mode perturbations whose gravitational equipotential surfaces have constant shape with time.

In order to test these approximations for non-symmetrical shapes, we compared them in the case of the collapse of a homogeneous ellipsoid. As expected from the results of Bertschinger & Jain (1994), we find that the NMA generically produces spindle-like singularities at collapse. The LTA, on the other hand, generically produces pancakes, just like the ZA. For triaxial ellipsoids, we compared numerical integrations of the local evolution equations with known solutions for a homogeneous ellipsoid in both cosmological and vacuum backgrounds. (An exact solution exists for the latter case while, in the former case, the homogeneous ellipsoid solution is not really exact because tides will cause the background, and then the ellipsoid itself, to become inhomogeneous. However, these effects are expected to be small.) We find that the LTA is significantly more accurate than the ZA (see Fig. 2).

These results suggest we have found a promising new approximation for nonlinear gravitational instability. However, we have only studied the evolution of isolated irrotational perturbations. Caution is needed because we do not know how accurate the LTA is for more general initial conditions, for example, those with vorticity. Moreover, we do not know by how much the tide produced by other mass elements degrades the accuracy. External tides modulate the equipotentials surrounding a mass element; qualitatively, we expect little effect as long as the external tide evolves weakly or is small compared with the trace part of the gravity gradient. Quantitative analysis is best done using N-body simulations, which we leave for later work.

The LTA has one significant limitation compared with the ZA. It tells us only the internal state of a given mass element (density, expansion rate, shear) and the tide on the element, but does not give the position of the element. However, for many purposes one cares more about the internal evolution of a mass element than about its position. For example, simple models of galaxy formation are based on spherical infall. These can be improved by inclusion of shear and tides (Bond & Myers 1993; Eisenstein & Loeb 1995). Our approximations could lead to even more accurate models of this sort. Also, if one

does need to know the positions of mass elements, then one can always supplement the Lagrangian fluid equations by the equation of motion for positions, perhaps using the Zel'dovich approximation or higher-order Lagrangian equations of motion. In principle, by following the velocity gradient for many mass elements, one can reconstruct the velocity field (up to an irrelevant overall constant), and then integrate the positions with $d\vec{x}/d\tau = \vec{v}$. An equivalent procedure was suggested by Matarrese et al. (1993).

Perhaps the most important reason for seeking new approximations like the LTA is that we still lack a good understanding of the behavior of collisionless systems under nonlinear gravitational instability. Future work will tell whether local Lagrangian flow methods will provide new insights.

Appendix: Second Order Calculation of M_{ij}

We write the Eulerian density fluctuation field $\delta = \delta^{(1)} + \delta^{(2)} + \ldots$ where $\delta^{(n)}$ is treated as being of nth order in perturbation theory. Similar expansions are used for the velocity field and the scaled gravitational potential

$$\hat{\phi} \equiv \frac{\phi}{4\pi G a^2 \bar{\rho}} = -\frac{1}{4\pi} \int d^3 x' \frac{\delta(\vec{x}\,')}{|\vec{x} - \vec{x}\,'|} \; . \tag{44}$$

For simplicity we shall assume an Einstein-de Sitter universe as in the numerical examples presented in this paper. In this case the perturbation series is a series in $a(\tau)$.

Peebles (1980) presents the result for $\delta^{(2)}$, which we rewrite using our variables as

$$\delta^{(2)} = \frac{5}{7} \left[\delta^{(1)} \right]^2 + \left[\vec{\nabla} \delta^{(1)} \right] \cdot \left[\vec{\nabla} \hat{\phi}^{(1)} \right] + \frac{2}{7} F^2 \; , \tag{45}$$

where $F^2 \equiv F^{ij} F_{ij}$ and

$$F_{ij} \equiv \nabla_i \nabla_j \hat{\phi}^{(1)} \; ; \tag{46}$$

note that $F^i{}_i = \delta^{(1)}$. From the Euler equation (2) we get the first and second order terms of the peculiar velocity,

$$\vec{v}^{(1)} = -\frac{\dot{a}}{a} \vec{\nabla} \hat{\phi}^{(1)} \; , \quad \vec{v}^{(2)} = -\frac{2}{5} \frac{\dot{a}}{a} \left[\vec{\nabla} \hat{\phi}^{(1)} \cdot \vec{\nabla} \right] \vec{\nabla} \hat{\phi}^{(1)} - \frac{3}{5} \frac{\dot{a}}{a} \vec{\nabla} \hat{\phi}^{(2)} \; , \tag{47}$$

where $\hat{\phi}^{(2)}$ is obtained using equation (44) with $\delta^{(2)}$.

We get M_{ij} and $-\nabla_k\, \epsilon^{kl}_{\ (i}H_{j)l}$ from equation (23). They vanish in first order; the second order results are

$$M_{ij} = 4\pi G\bar\rho a\dot a\left\{\delta^{(1)}F_{ij} - \frac{7}{5}\nabla_i\nabla_j\hat\phi^{(2)} + \frac{7}{5}\left[\vec\nabla\hat\phi^{(1)}\cdot\vec\nabla\right]F_{ij} + \frac{2}{5}F^k_{\ (i}F_{j)k}\right\}\ ,\qquad (48)$$

$$-\nabla_k\,\epsilon^{kl}_{\ (i}H_{j)l} = M_{ij} + 4\pi G\bar\rho a\dot a\left\{3\delta^{(1)}F_{ij} - 3F^k_{\ (i}F_{j)k} + \delta_{ij}\left(F^2 - \left[\delta^{(1)}\right]^2\right)\right\}\ .\qquad (49)$$

It can be verified that these quantities are traceless as expected using equations (45) and (46). In general, neither vanishes in second order perturbation theory.

REFERENCES

Bagla, J. S., & Padmanabhan, T. 1994, MNRAS, 266, 227

Barnes, A., & Rowlingson, R. R. 1989, Class. Quantum Gravity, 6, 949

Barrow, J. D., & Saich, P. 1993, Class. Quantum Gravity, 10, 79

Bertschinger, E. 1995, in Cosmology and Large Scale Structure, proc. Les Houches XV Summer School, in press

Bertschinger, E., & Hamilton, A. J. S. 1994, ApJ, 435, 1

Bertschinger, E., & Jain, B. 1994, ApJ, 431, 486

Bond, J. R., & Myers, S. T. 1993, preprint

Brainerd, T. G., Scherrer, R. J., & Villumsen, J. V. 1993, ApJ, 418, 570

Bruni, M., Matarrese, S., & Pantano, O. 1995, ApJ, 445, 958

Buchert, T. 1993, A&A, 267, L51

Coles, P., Melott, A. L., & Shandarin, S. F. 1993, MNRAS, 260, 765

Ehlers, J. 1961, Akad. Wiss. Lit. Mainz Abh. Math.-Nat. Kl. 11

Eisenstein, D. J., & Loeb, A. 1995, ApJ, 439, 520

Ellis, G. F. R. 1971, in General Relativity and Cosmology, ed. R. K. Sachs (New York: Academic), 104

Fillmore, J. A., & Goldreich, P. 1984, ApJ, 281, 1

Icke, V. 1973, A&A, 27, 1

Kofman, L. 1991, in Primordial Nucleosynthesis and Evolution of Early Universe, ed. K.
    Sato & J. Audouze (Dordrecht: Kluwer), 495

Kofman, L., & Pogosyan, D. Yu. 1995, ApJ, 442, 30

Kofman, L., Pogosyan, D. Yu., & Shandarin, S. F. 1990, MNRAS, 242, 200

Ehlers, J. 1961, Akad. Wiss. Lit. Mainz Abh. Math.-Nat. Kl. 12

Lin, C. C., Mestel, L., & Shu, F. H. 1965, ApJ, 142, 1433

Matarrese, S., Lucchin, F., Moscardini, L., & Saez, D. 1992, MNRAS, 259, 437

Matarrese, S., Pantano, O., & Saez, D. 1994, Phys. Rev. D, 47, 1311

Melott, A. L., Buchert, T., & Weiss, A. 1995, A&A, 294, 345

Peebles, P. J. E. 1980, The Large Scale Structure of the Universe (Princeton: Princeton
    University)

Sachs, R. 1961, Proc. Roy. Soc. London, 264, 309

White, S. D. M., & Silk, J. 1979, ApJ, 231, 1

Zel'dovich, Ya. B. 1970, A&A, 5, 84

Zel'dovich, Ya. B., & Novikov, I. D. 1983, The Structure and Evolution of the Universe
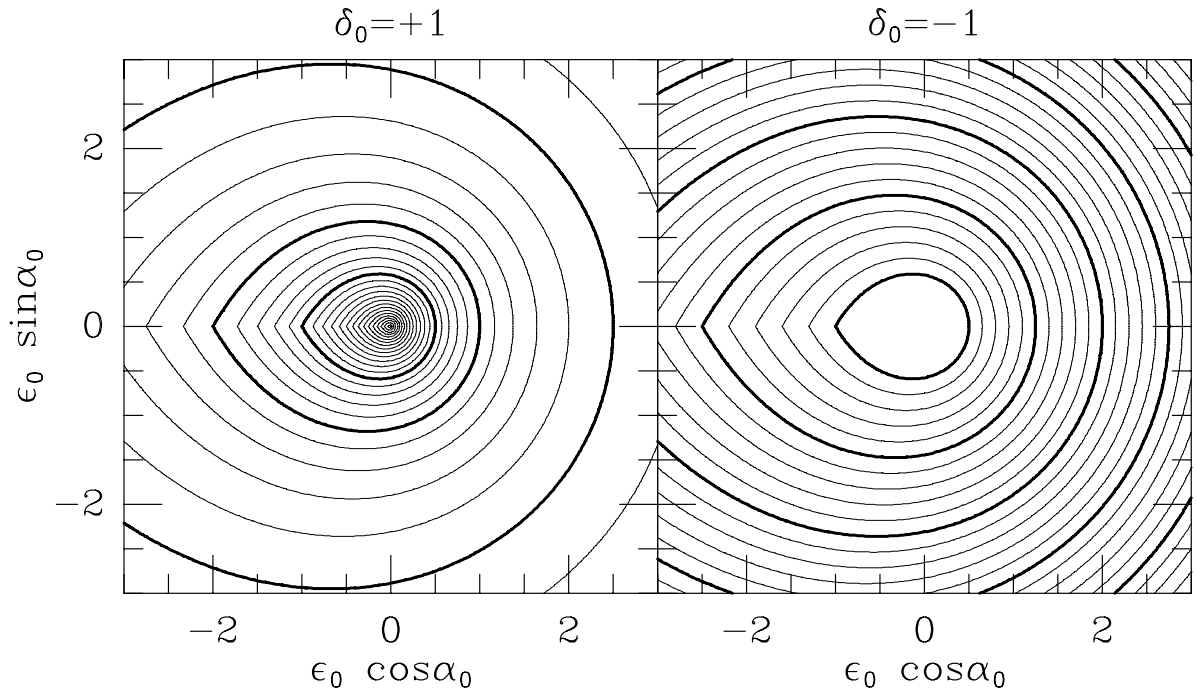   (Relativistic Astrophysics, volume 2) (Chicago: University of Chicago Press)

Fig. 5a.— Contours of constant collapse time computed using the ZA, expressed by the cosmic expansion factor a_c or its reciprocal, versus initial tidal field parameters. Left panel: initial positive density perturbations. The light (heavy) contours are spaced by 0.1 (0.5) in a_c, with the outermost contour $a_c = 0.4$ and the central value (corresponding to spherical collapse) $a_c = 3.0$. The ZA significantly overestimates the collapse time for low-shear perturbations. Right panel: initial negative density perturbations. The light (heavy) contours are spaced by 0.1 (0.5) in a_c^{-1}, with the innermost contour $a_c^{-1} = 0$ and the outermost one $a_c^{-1} = 2.3$. Initial perturbations in the central region do not collapse. Perturbations are oblate (prolate) for $\epsilon_0 \cos \alpha_0 > 0$ ($\epsilon_0 \cos \alpha_0 < 0$).
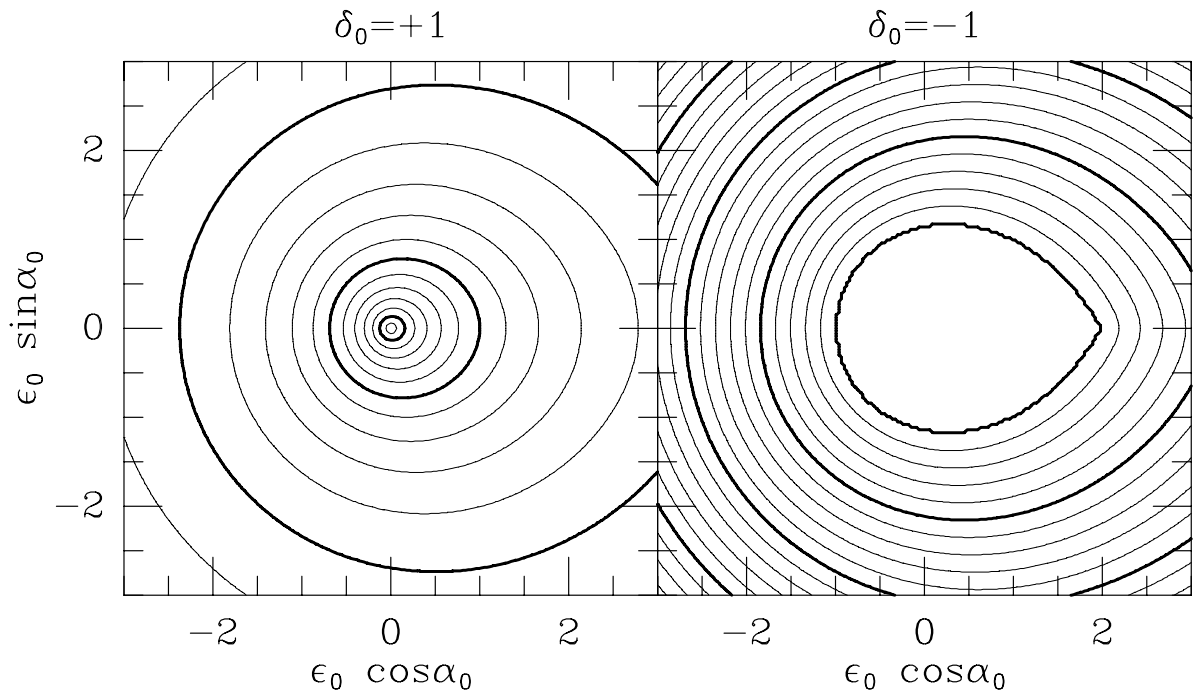
Fig. 5b.— Same as Fig. 5a except that the NMA is used. In the left panel the innermost contour is $a_c = 1.6$. In the right panel the outermost contour is $a_c^{-1} = 1.8$. The smaller extent of the contours for prolate configurations $(\epsilon_0 \cos \alpha_0 < 0)$ reflects the fact that the NMA favors prolate collapse.
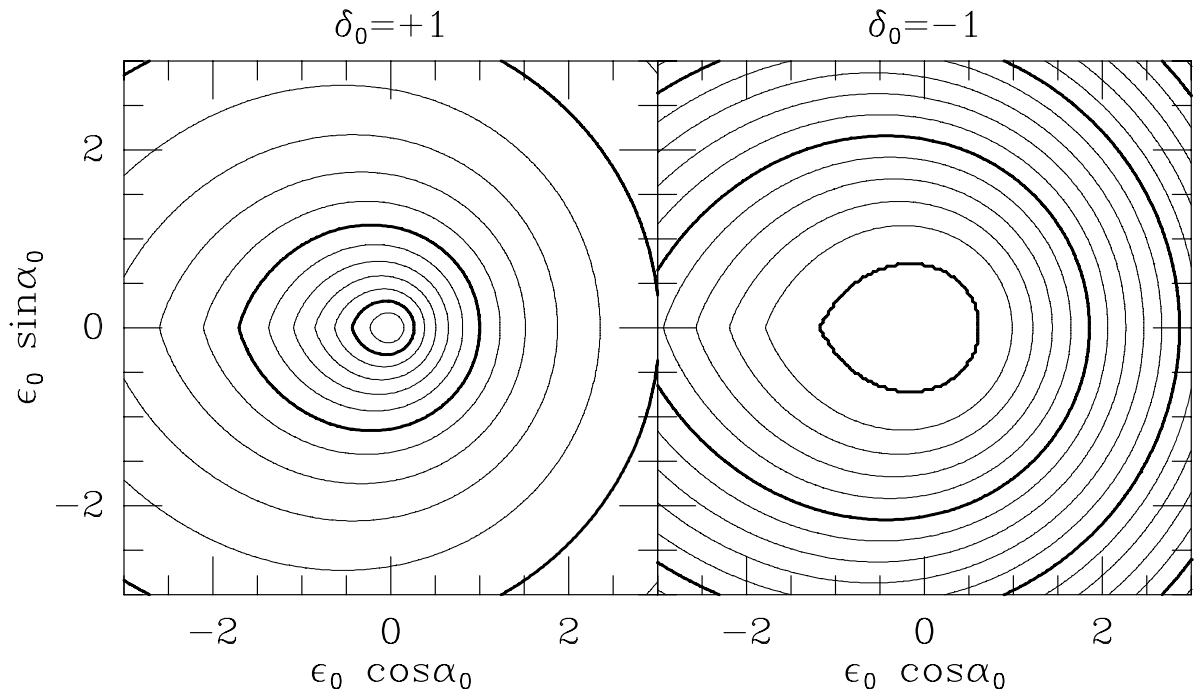
Fig. 5c.— Same as Fig. 5a except that the LTA is used. In the left panel the innermost contour is $a_c = 1.6$. In the right panel the outermost contour is $a_c^{-1} = 1.6$. The LTA, like the ZA, favors oblate (pancake) collapse over prolate (spindle) collapse.